Supplement of The Cryosphere, 14, 565–584, 2020
https://doi.org/10.5194/tc-14-565-2020-supplement

The Cryosphere Open Access EGU

Supplement of

Deep learning applied to glacier evolution modelling

Jordi Bolibar et al.

Correspondence to: Jordi Bolibar (jordi.bolibar@univ-grenoble-alpes.fr)

1. Filtering of DEM rasters

Before computing the glacier-specific Δh parameterized functions, some preprocessing is done to the regional French Alps DEM raster files in order to filter artefacts and noise. The processing chain works as follows:

1. The regional DEM files are cropped using the 2003 glacier inventory shapefile outlines, thus obtaining glacier-specific rasters with the DEMs from 1979 and 2011.
2. The glacier surface altitude difference for this period (so-called dh/dt) which corresponds to the change in ice thickness is computed glacier by glacier by subtracting the two previously mentioned DEM rasters.
3. A first empirical filter is applied to all rasters to filter unrealistic values coming from artefacts (*e.g.*, presence of clouds or saturation on the images used to generate de DEMs).
4. The filtered ice thickness difference (dh/dt) and DEM rasters are paired together as in Figure S3, and a low-order polynomial fit is applied in order to get the main trend of the scatterplot between the ice thickness difference *vs.* altitude.
5. A dynamic envelope/buffer around the polynomial fit line is computed for each glacier based on a quantile between maximum and minimum values for each altitude. In order to smooth the computed envelope for each altitude, a convolutional filter is applied to these values in order to smooth them and to follow the polynomial fit. A dynamic sliding window size is used to adjust the averaging process to the characteristics of each glacier.
6. A second filter is then applied using the computed smoothed envelope buffer to remove outliers
7. A final polynomial fit is computed with a variable order depending on the number of remaining data values of each glacier.
8. The percentage of pixels of information available for computing the polynomial fit (the parameterized function) is displayed for each glacier at the end of the processing chain.

2. SMB statistical error analysis

In order to determine the error due to each predictor, a Lasso model was trained with the same training matrix as the ANN, but instead of using SMB as ground truth data the errors generated by the ANN without weights were used. As discussed in section 4.1, Lasso performs a regularization on the training dataset, thus keeping only certain predictors and removing the rest. By looking at the resulting coefficients of the model, we can estimate the linear contribution of each predictor to the final model error. Latitude and longitude appear as the most important error predictors, but their contribution might in fact indicate the different magnitude of errors between glaciers or regions, since the pair of coordinates specifically identifies each glacier. October, August and March temperature follow behind, indicating that changes in temperature during these months have an influence in the simulation errors. It is not surprising that two of these months appear as top predictors as seen in Fig. 5 as changes in temperature during these months at the transition between the accumulation and ablation season can have a strong importance on the surface mass balance processes.

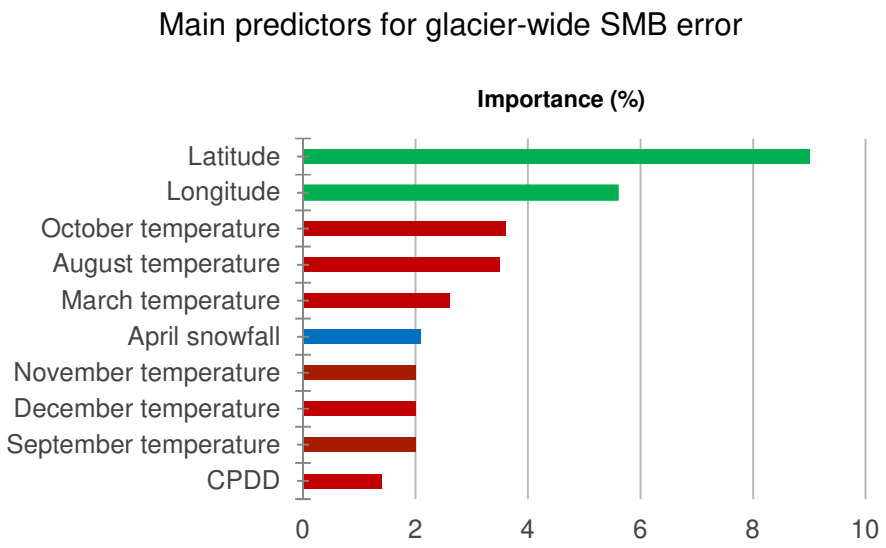

Figure S1: Importance (%) of the first 10 predictors using Lasso to predict residual error from the ANN SMB model. Green bars indicate topographical features, red bars temperature-related features and blue bars precipitation-related features.

Such an approach to analyze the influence of the different predictors into the quantification of uncertainties is of course limited, since a linear model is trained with nonlinear results. But these results are useful to determine the main contributors to errors rather than quantifying these errors, which has been done with the LOGO, LOYO and LSYGO cross-validations.

3. Topographical glacier-wide SMB predictors

Since topography plays a role in the glacier-wide SMB signal, besides the climate, the representation of the glacier's topography is important in order to correctly simulate its glacier-wide SMB and its geometrical evolution. As explained in Sect. 2.1 "Model overview and workflow" and Sect. 3.1.2 "Topographical glacier data and altimetry", the source of the topographical predictors used for the simulation of glacier-wide SMB is different at different steps of the glacier evolution simulation chain. Two cases exist:

1. For the machine learning training of the glacier-wide SMB models, which is performed on historical data, all topographical data comes from the multitemporal glacier inventories (Gardent et al., 2014, with 2015 update). In order to have an annual timestep, topographical data from these inventories are linearly interpolated.
2. For the full glacier evolution simulation, coupling the glacier-wide SMB component with the glacier geometry evolution component, the model must be capable of generating all the input topographical predictors even for non-observed glaciers and future periods. For every glacier and year, all the topographical predictors are computed from the updated glacier-specific ice thickness and DEM raster files from Farinotti et al. (2019), which

then are used to simulate a single glacier-wide SMB for that glacier and year. Then, this glacier-wide SMB together with the glacier-specific geometry update function are used to update the glacier's geometry and their respective ice thickness and DEM rasters. For the next year, all the topographical predictors are recomputed with the updated raster files, and this process is repeated in a loop with an annual timestep. Therefore, the glacier-wide SMB model is called with an annual timestep, simulating only single values in order to take into account the evolution of the glacier's topography.

In order to show that the glacier geometry update component, coupled with the glacier-wide SMB simulation component can successfully simulate the evolution of the topographical characteristics of glaciers in the region, a specific test was designed. Using the same validation period as in Sect. 3.2 (2003-2015), we ran parallel simulations of glacier-wide SMB for all the 32 case study glaciers. The first simulation was done using case (1), with the multitemporal glacier inventories data, and the second one was done following case (2), with the full glacier evolution model and the Farinotti et al. (2019) raster files. The results of both simulations were really similar, revealing only small differences. On average, the simulated glacier-wide SMBs for this period differed on 0.069 m.w.e. a^{-1}, due to the differences in the input topographical predictors, which are computed from different datasets (Fig. S6). Moreover, the performances of both simulations for this period are very similar, with a RMSE of 0.49 m.w.e. a^{-1} for case (1) and 0.52 m.w.e. a^{-1} for case (2). The results with all the differences between the simulated glacier-wide SMB values and input topographical values are summarized in Table S1:

Variable (multitemporal inventories vs. full glacier evolution)	**SMB simulated**	**Slope**	**Average glacier elevation**	**Area**
MAE or mean difference	0.069 m.w.e a^{-1}	1.8°	31.3 m	0.2 km^2

Table S1: Differences on simulated glacier-wide SMB and topographical predictors between a simulation using interpolated topographical predictors from the multitemporal glacier inventories and the full glacier evolution simulations including the coupling of the glacier-wide SMB with the glacier geometry update.

The only striking difference is perhaps the difference in simulated areas. This is mainly due to the fact that the Farinotti et al. (2019) dataset uses the RGI v6, which for the largest glaciers of Argentière and Mer de Glace, overestimates its surface area (from 32 to 34 km^2 for Mer de Glace in 2003). The differences in slope are explained by the fact that this variable is not included in the multitemporal glacier inventories (Gardent et al., 2014), therefore it has been computed once with a global DEM and kept constant for each glacier throughout the years for the training of the SMB model. On the other hand, in order to include the long term effects of glacier morphology changes in the glacier evolution simulations (glacier-wide SMB simulation + glacier geometry update), the glacier slope is re-computed with an annual timestep and it evolves through time. Therefore, there are small differences for certain glaciers whose slope has evolved during this period, thus accounting for the differences with the fixed value used for the training of the SMB model.

This test serves to prove that the full glacier evolution simulations in ALPGM are capable of reproducing the topographical predictors used for the training of the glacier-wide SMB machine learning models. Moreover, this test also helps to prove that ALPGM can correctly simulate the topographical evolution of glaciers, which allows to capture the topography induced feedback, which plays a role in the simulation of glacier-wide SMBs.

4. Supplementary figures

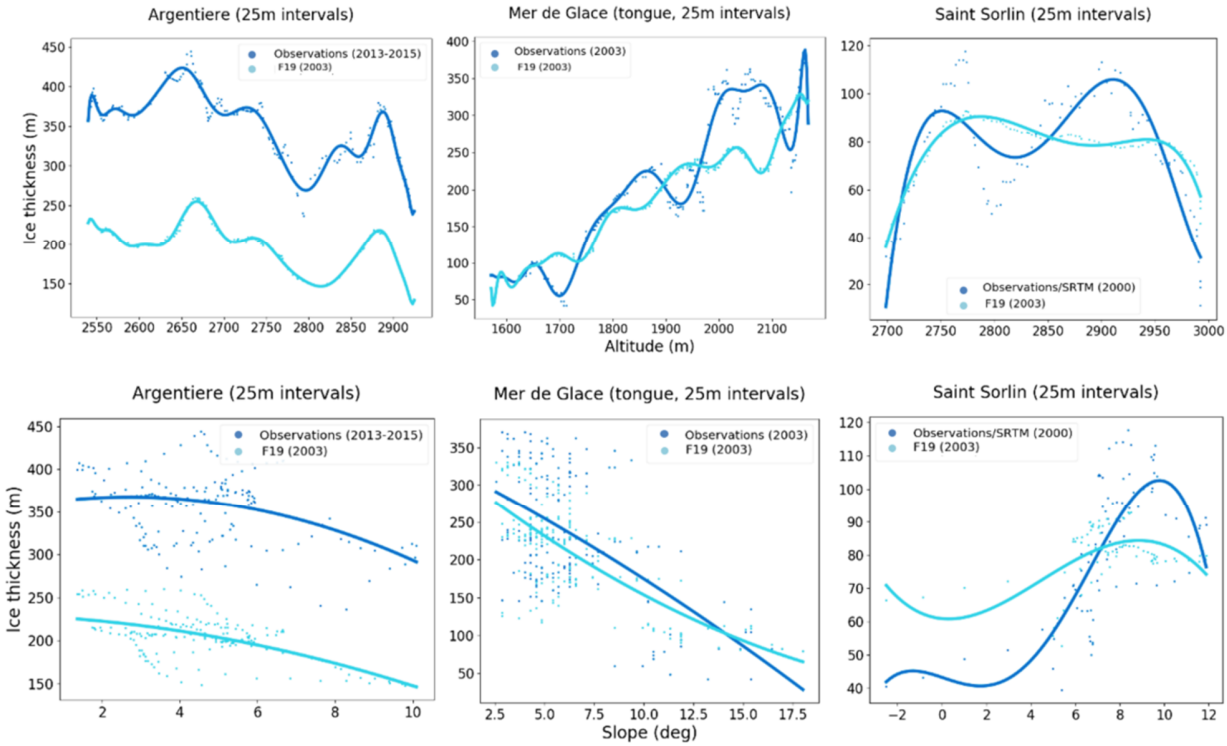

Figure S2: Comparison of simulated glacier ice thicknesses from F19 with observations from the GLACIOCLIM observatory. Points are compared at 25 m intervals on the glacier flowline. The polynomial fits have less degrees of freedom for the slope plots. Note that for some glaciers the dates are not the same

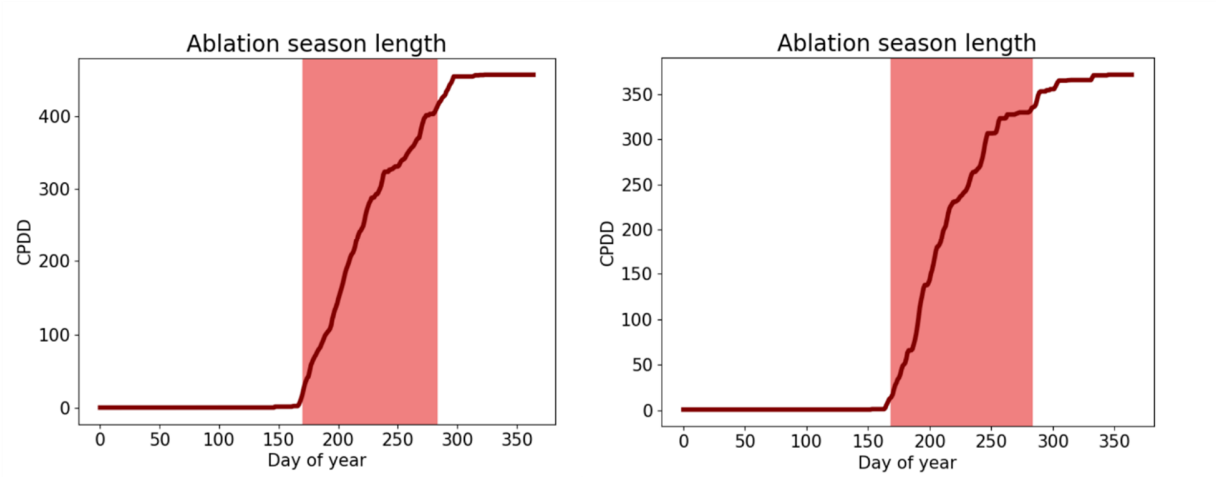

Figure S3: Example of dynamical calculation of ablation season length used for computing the annual CPDD value for Glacier Blanc (Écrins cluster) in 1963 (left) and 1984 (right)

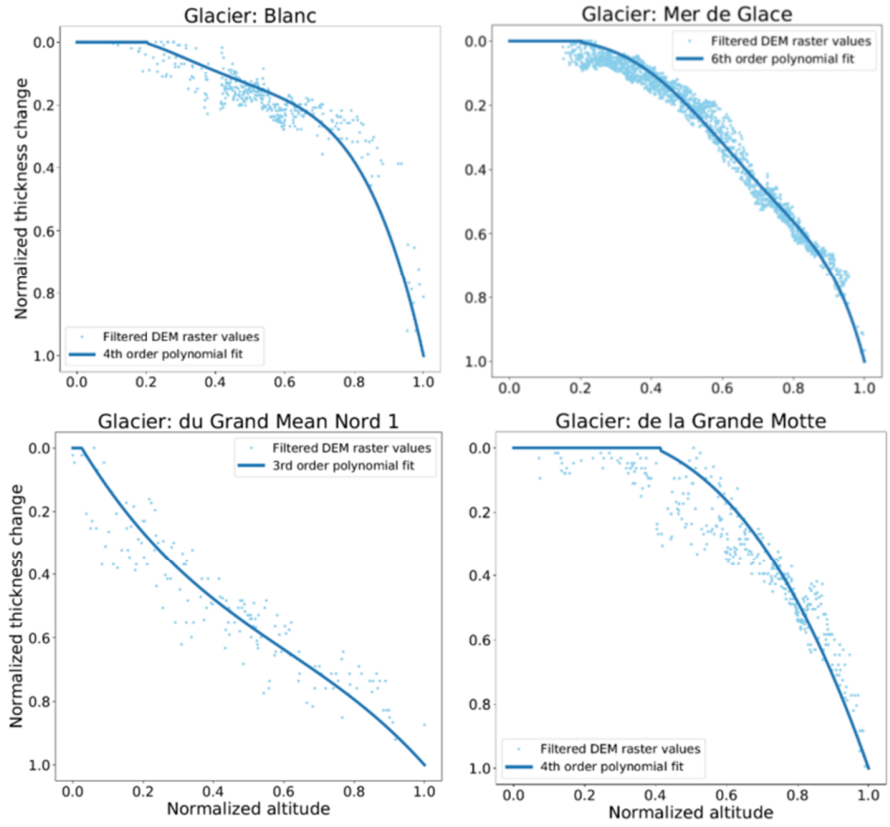

Figure S4: Examples of glacier specific Δh parameterized functions generated by ALPGM. The order of the polynomial fit depends on the number of available pixels.

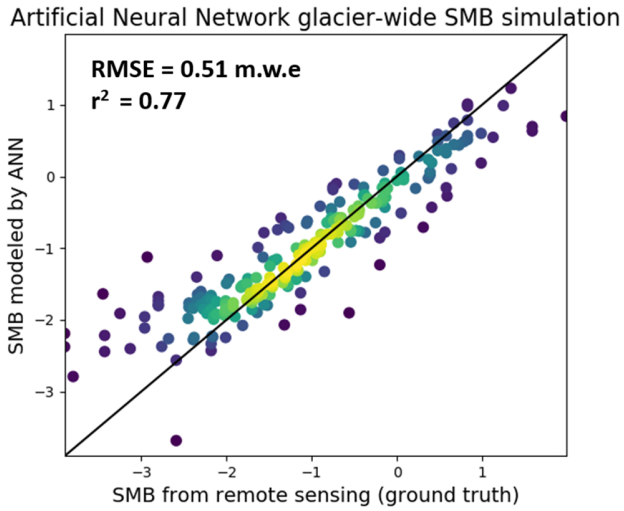

Figure S5: Results for the spatiotemporal cross-validation using Leave-Some-Glaciers-and-Years-Out (LSYGO). SMB values are in m.w.e. Compared to the other scatter plots from 3.2, there are less values available for test due to the severity of the spatiotemporal independence.

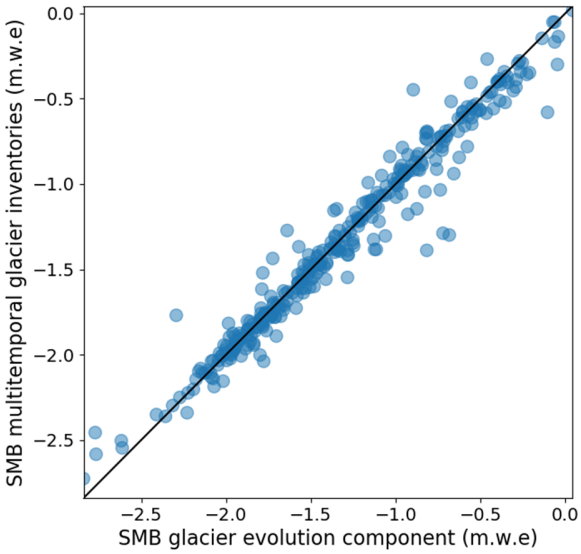

Figure S6: Comparison of glacier-wide SMB simulations (2003-2015, 32 case study glaciers) using topographical predictors from the multitemporal glacier inventories (Y axis) vs. using the full glacier evolution simulations in ALPGM with the Farinotti et al. (2019) ice thickness and DEM rasters (X axis). Average difference = 0.069 m.w.e. a^{-1}

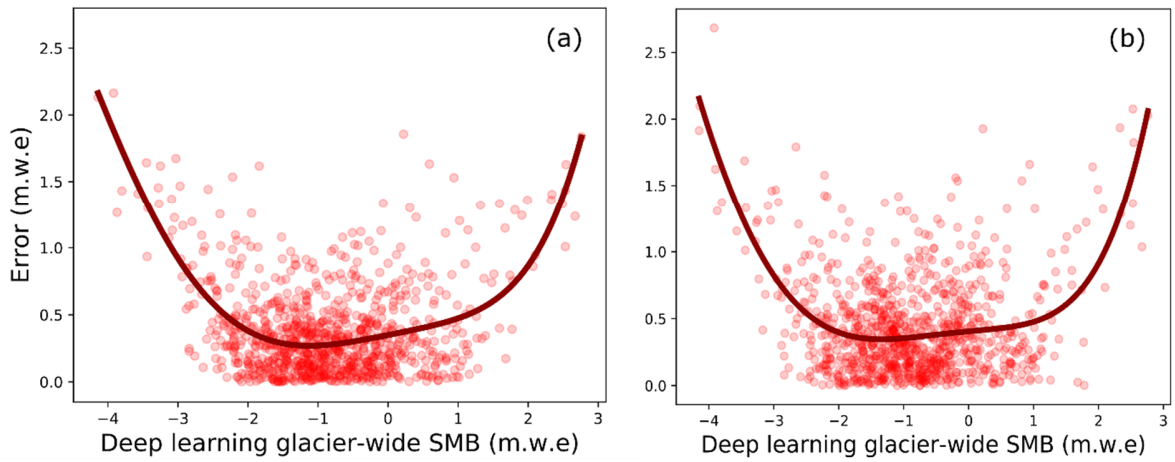

Figure S7: Error distribution of deep learning (without weights) glacier-wide SMB simulations for the 1984-2015 period for the 32 case study glaciers. (a) Performance in the spatial dimension using LOGO cross-validation; (b) performance in the temporal dimension using LOYO cross-validation. The red line corresponds to a 5th order polynomial fit.